УДК 621.793.74
DOI: 10.33184/bulletin-bsu-2023.3.5

ANALYSIS OF THE TURBULENCE INFLUENCE IN THE ELECTRIC ARC PLASMA FLOW BY THE LABORATORY STUDY METHOD

© D. S. Kriskovets, V. Ya. Frolov, B. A. Yushin

Peter the Great St. Petersburg Polytechnic University
29 Polytechnicheskaya Street, 195251 St. Petersburg, Russia.

Email: dkriskovets@gmai.com

This paper refers to the combined study of the influence of plasma flow turbulization degree on the efficiency of the plasma spraying technological process. The basis of the study is the absence of consensus between two optimization approaches, which are used to increase the profitability of plasma systems for coating, applying by the groups of scientists, who prefer laminar or turbulent plasma flow gear.

The study contains: mathematical model of the heat exchange between the metal particle and plasma flow with the variation of process parameters – flow character and the dimensions of the boarder layer, which depends from the turbulization degree, controlled by the exchange of the two perpendicularly directed parts of the flow speed; laboratory performance research experiences of the plasma spraying system with the variation of the material and flow turbulization degree, which have been controlled with the help of an innovative technique. The astounding results reduce the opinions of the mainstream scientific schools into the union point, showing that the most optimal mode for the operation of plasma devices is exploitation with the flow in condition of the laminar-turbulent transition.

Keywords: *plasma, spraying, coating, flow, turbulent, laminar.*

Introduction

Plasma spraying, which was born as the evolution of metallization flame spray process 1, has a significant drawback, compared to its progenitor 2, which greatly limits the widespread introduction of this technology 3 – a high degree of energy consumption of the process (low efficiency).

A lot of great scientists and engineers have tried to modernize the technological process of plasma spraying for many years, constantly working on equipment improving 4, trying different approaches 5. At the moment, the main way to increase the efficiency of this process is to use plasma torches, which generate long plasma jets with laminar character of the flow – the method, which increase the amount of time of the melted particle in a high-temperature zone 6. However, there is a large number of scientists 7, who follow the theory, according to which, an increase of flow turbulization degree is considered as a catalyst for the emergence of optimal conditions for the implementation of heat transfer during the plasma spraying process, and, probably, the main reason for this is the increase of viscous dissipation parameter 8.

The turbulent nature of the heat exchange between the plasma forming gas and the arc column leads to an increase in high-frequency pulsations (the amplitude and frequency of which depend upon the flow rate), composition, gas temperature, shunting dynamics of the arc column. These pulsations cause the fluctuations in the enthalpy, temperature, velocity of the plasma jet with frequencies up to several kilohertz. There is an assumption, that during the heat transfer in a turbulent flow, the heat transfer coefficient α increases, since the boundary layer that hinders the heat exchange between plasma and particle (an area with multiple growing of the viscosity parameter and the big recession of the thermal conductivity) dissipates much more intensively, than in the case of the laminar outflow, under the influence of the multidirectional forces.

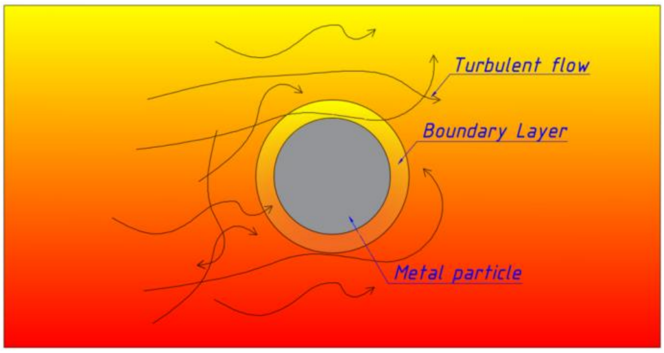

Figure 1. Visualization of the influence of turbulent flow on the geometric characteristics of the boundary layer.

Study methodology

To indicate the conclusions about the feasibility of the above concept, it is necessary to conduct a series of experiments, the methodology of which is aimed at setting and solving of engineering optimization task for the plasma spraying process.

The dimensionless complex, called the Reynolds criterion, is the criterion for the similarity of gas dynamic flows and in the case under consideration is defined as 9:

$$\mathrm{Re} = \frac{\rho_{gas} \cdot v_p \cdot d}{\mu}, \quad (1)$$

where ρ_{gas} – density of the plasma, v_p – plasma flow velocity in the zone of nozzle outlet, d – nozzle diameter, μ – dynamic viscosity of the plasma.

According to Klubnikin 10, the occurrence of turbulence in the flow inside a cylindrical tube (the shape of the plasma torch channel) corresponds to the value of the Reynolds number ≈ 800.

The Prandtl number, constructed from the physical properties of the environment (c_p – heat capacity, λ – thermal conductivity, μ – dynamic viscosity) characterizes the thermophysical properties of the coolants.

$$\mathrm{Pr} = \frac{\mu \cdot c_p}{\lambda}. \quad (2)$$

The Reynolds and Prandtl numbers determine the dimensions of the dynamic boundary layer δ_v (the layer, where the area velocity changes from the value at the outer boundary with the plasma to 0 at the particle outer boundary) and the temperature boundary layer δ_T (the layer, where the area temperature varies from the value at the outer boundary with the plasma to the value at the particle outer boundary) 9:

$$\delta_v = \frac{d_s}{\sqrt{\mathrm{Re}}}, \quad (3)$$

$$\delta_T = \frac{d_s}{\sqrt{\mathrm{Re}} \cdot \sqrt{\mathrm{Pr}}}, \quad (4)$$

where d_s is the average particle diameter.

To set and solve the optimization problem, there is a mathematical apparatus that allows us to vary all the available parameters, and the laboratory application that allows us to change only the following ones 10: voltage, current strength, plasma forming gas flow velocity (plasma forming gas mass flow rate), feed velocity of the powder material (powder mass flow rate).

Through the mathematical modelling the target function in the process of optimization task solving will be the maximum value of the efficiency. Based on 7, it follows:

$$\eta = \frac{P_1}{P} = \frac{\alpha \cdot \Delta T \cdot \frac{l_j}{v_p} \cdot S}{U \cdot I \cdot (m \cdot n / G)} = \frac{\alpha \cdot \Delta T \cdot l_j \cdot \left(\frac{G}{\rho_{pow} \cdot \frac{4}{3}(\pi R^3) \cdot (n)} \cdot 4 \cdot \pi \cdot R^2 \cdot (n)\right)}{U \cdot I \cdot \left|\overrightarrow{v_{pow}} - \overrightarrow{v_g}\right|}, \quad (5)$$

where P – total power expended, P_1 – is the power, expended on the powder heating, ΔT– is the difference between plasma temperature and the temperature, which supplied to the heated particles, l_j – is the length of the plasma jet thermal active zone, $\overrightarrow{v_{pow}}$ – velocity of the powder supply, $\overrightarrow{v_g}$ – velocity of the plasma forming gas, α – heat transfer coefficient, S – particles surface (in the amount of $n = \frac{G \cdot t}{\rho_{pow} \cdot \frac{4}{3}(\pi R^3)}$ by the time t), m – mass of the particles, G – the mass flow rate of the powder material, ρ_{pow} – the bulk density of the material, R – is the radius of the particle.

During the laboratory study the target function in the process of the optimization task solving will be the maximum value of the process performance:

$$W = \frac{\Delta m}{t}, \quad (6)$$

where Δm is the mass increase of the substrate after coating, t is the coating application time.

For the convenience of correlation of the experiments results, in each of the study approaches the same parameters are varied and the same functional restrictions are imposed on both researches.

For the mathematical and the real experiments realization, it is possible to vary all the following parameters: $G = v_{pow} \cdot S_1 \cdot \rho_{pow}$ – powder mass flow rate, so v_{pow} – within the range from 10 to 100 m/s; $G' = v_g \cdot S_2 \cdot \rho_{gas}$ – flow rate of the plasma forming gas, so v_g – within the range from 50 to 200 m/s; Reynolds number Re (the character of the gas flow movement), it is the calculated parameter for each case, and it directly depends from the plasma flow velocity, temperature, nozzle diameter – it has a significant impact on the value of the α parameter; arc voltage U – within the range from 100 to 200 V; arc current I – within the range from 100 to 200 A.

The functional limitations of this experiment are the following: inability of plasma torch geometric parameters control ($S_c = 6 - 8\ \mathrm{mm}^2, l_c = 300\ \mathrm{mm}$); constant spraying application time (t = 8 s); constant end equal power values in the experiments on the study of laminar and turbulent flows (P = const. = 24 000 W); constant temperature and dimensions of the plasma arc central part (T = 6 000 K; $\mathrm{Pr} = \frac{\mu \cdot c_p}{\lambda} = 0.54$); constant l – distance to the surface of the workspace – allows us to reduce the length of the jet, equal to the summary of its channel and outer parts $l_j = l_c + l_{od} = 350\ \mathrm{mm},\ \text{if}\ l_c \le l$. For modeling and the laboratory experiment the powdered metal (Al, Ni3Al) will be used with fraction, which is equal to 60 microns.

Mathematical modeling for the technological process optimization

The mathematical model of the processes occurring in the plasma torch is based on a several fundamental laws 8.

Law of the energy conservation (energy balance equation):

$$\rho c_P\left(v_z\frac{\partial T}{\partial z}+v_r\frac{\partial T}{\partial r}\right)=\sigma E^2-U_{rad}+\frac{\partial}{\partial z}\left(\lambda\frac{\partial T}{\partial z}\right)+\frac{1}{r}\frac{\partial}{\partial r}\left(\lambda\frac{\partial T}{\partial r}\right), \quad (7)$$

where σ is the electrical conductivity of the plasma; E is the electric field strength; U_{rad} is the plasma radiation; v_z, v_r are the axial components of the plasma velocity.

Maxwell's laws:

$$\begin{cases} div\vec{B}=0 \\ rot\vec{H}=\vec{J} \\ rot\vec{E}=-\frac{\partial B}{\partial t} \\ div\vec{E}=\frac{\rho}{\varepsilon} \end{cases}, \quad (8)$$

where $\vec{B}$ is the magnetic induction, $\vec{H}$ is the magnetic field strength, $\vec{J}$ is the current density, ε is the absolute permittivity.

Constitutive equations:

$$\vec{J}=\ \vec{E}; \quad (9)$$

$$\vec{B}=\ \mu_0\vec{H}; \quad (10)$$

$$\vec{D}=\ \varepsilon_0\vec{E}, \quad (11)$$

Where $\vec{D}$ is electric induction, μ_0 magnetic permeability of the vacuum, ε_0 vacuum permittivity.

Motion equations (law of the momentum conservation):

$$v_z:\rho\left(v_z\frac{\partial v_z}{\partial z}+v_r\frac{\partial v_z}{\partial r}\right)=\frac{\partial}{\partial z}\left(\mu\frac{\partial v_z}{\partial z}\right)+\frac{1}{r}\frac{\partial}{\partial r}\left(r\mu\frac{\partial v_z}{\partial r}\right)-\frac{\partial p}{\partial z}+F_{Bz}+\rho g_z; \quad (12)$$

$$v_r:\rho\left(v_z\frac{\partial v_r}{\partial z}+v_r\frac{\partial v_r}{\partial r}-\frac{\partial v_\varphi^2}{2r}\right)=\frac{\partial}{\partial z}\left(\mu\frac{\partial v_r}{\partial z}\right)+\frac{1}{r}\frac{\partial}{\partial r}\left(r\mu\frac{\partial v_r}{\partial r}\right)-\frac{\partial p}{\partial r}+F_{Br}-\mu\frac{v_\varphi}{r^2}; \quad (13)$$

$$v_\varphi:\rho\left(v_z\frac{\partial v_\varphi}{\partial z}+v_r\frac{\partial v_\varphi}{\partial r}-\frac{v_\varphi v_r}{r}\right)=\frac{\partial}{\partial z}\left(\mu\frac{\partial v_\varphi}{\partial z}\right)+\frac{1}{r}\frac{\partial}{\partial r}\left(r\mu\frac{\partial v_\varphi}{\partial r}\right)+F_{B\varphi}-\mu\frac{v_\varphi}{r^2}, \quad (14)$$

where v_φ is the angular component of the plasma velocity; μ is the dynamic viscosity in the vacuum; F_{Bz}, F_{Br}, $F_{B\varphi}$ are the components of the magnetic pressure force; $\frac{\partial p}{\partial z}$, $\frac{\partial p}{\partial r}$ are the gas static pressure gradients; ρg_z is the gravity force.

Continuity equation (law of the mass conservation):

$$\frac{\partial}{\partial z}(\rho v_z)+\frac{1}{r}\frac{\partial}{\partial r}(r\rho v_r)=0. \quad (15)$$

The "COMSOL Multyphysics" calculation system, the materials data from the application material library and the build-in calculation modules were used for the development of the mathematical model.

Based on the absence of need for a detailed consideration of all the processes occurring in plasma arcs (during the initial study of the influence of the movement nature of the gaseous environment on the heat exchange between the plasma and the powder material), the problem is reduced to calculating the thermodynamics in the space, which surrounds the metal particle.

Table 1 shows the results of calculations of the dynamic boundary layer and the temperature boundary layer. To simplify the further calculations, the average size of the boundary region δ_{av} and the color indication of the nature of gas movement (green for the laminar flow and red for the turbulent flow) were introduced. The values were found by using of data from the preliminary analytical R_e и P_r calculation (formulas *(1–2)*). Data from *Table* 1 directly affect on the formulation of every subtask of thermodynamic process study.

To set the task the standard calculation modules for the "COMSOL Multyphysics" application were used. The block diagram of the study statement is shown on the 0.

Calculation modules: "Laminar Flow (spf)"; "Turbulent Flow, k-ε"; "Heat Transfer in Solids and Fluids"; "Noniso-thermal Flow".

Materials: "Aluminum [solid]" – aluminum particle; "Air_1 [gas]" – plasma forming gas – air with properties for 6 000 K temperature condition; "Air_2 [gas]" – boundary layer (plasma forming gas zone with 1.5× increased value of dynamic viscosity and a reduced in 2 times value of thermal conductivity.

For modeling a primitive 3-D geometry is used. It simulates the heat exchange system under consideration, which includes two spheres and cube. The smaller sphere (with a diameter of 60 μm) is aluminum particle. A large sphere (with a diameter equal to 60 + δcp μm, according to the 0) is the boundary layer. The cube is a part of the plasma jet space, the size of the cube face is 500 μm. Boundary and initial conditions are indicated by callouts and inscriptions on the *Fig.* 2.

The desired values are the average temperatures of the particle, boundary layer and the plasma flow at the different ratios of the velocities of the plasma forming gas and powder material supply. They are displayed in the form of color maps (*Fig*. 3). An analysis of the calculation results makes it possible to compile the tables of values for the distribution of average temperature indicators inside the study area.

Table 1

Calculation of the boundary layer geometric parameters

Vpow/Vg	50	100	150	200
Re				
25	318.48	587.24	866.35	1148.29
50	402.85	636.96	900.79	1174.49
75	513.53	712.14	955.43	1216.90
100	636.96	805.69	1027.06	1273.91
δv, μm				
Vpow/Vg	**50**	**100**	**150**	**200**
25	3.36	2.48	2.04	1.77
50	2.99	2.38	2.00	1.75
75	2.65	2.25	1.94	1.72
100	2.38	2.11	1.87	1.68
δT, μm				
Vpow/Vg	**50**	**100**	**150**	**200**
25	4.55	3.35	2.76	2.39
50	4.04	3.21	2.70	2.37
75	3.58	3.04	2.62	2.33
100	3.21	2.86	2.53	2.27
δav, μm				
Vpow/Vg	**50**	**100**	**150**	**200**
25	3.95	2.91	2.40	2.08
50	3.52	2.80	2.35	2.06
75	3.11	2.64	2.28	2.02
100	2.80	2.49	2.20	1.98

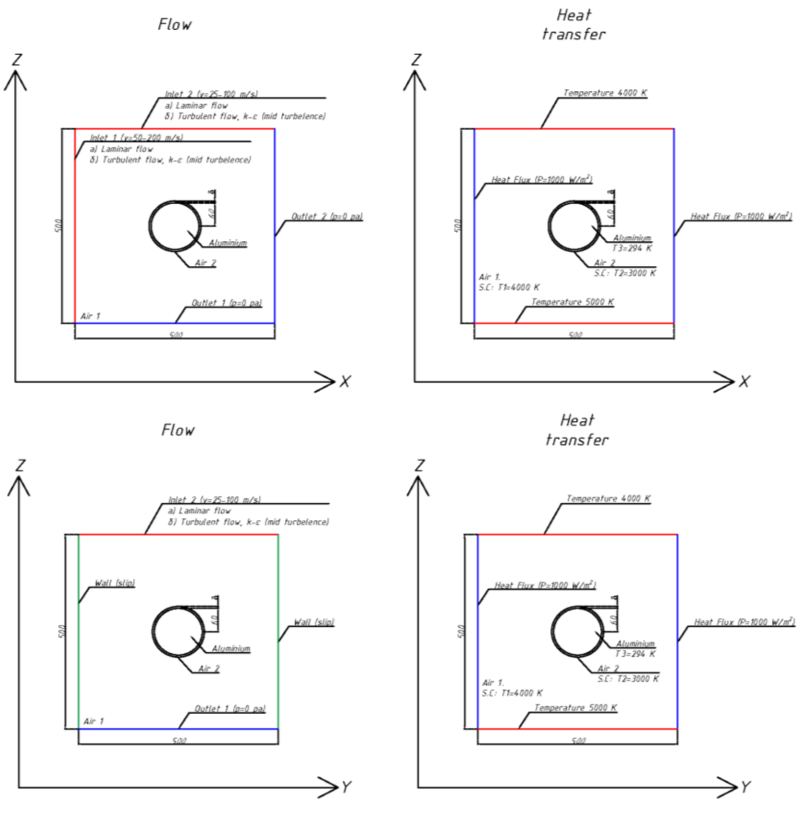

Fig. 2. The set of the study.

The calculation results (*Table* 2) showed, that the most efficient parameters of the heat exchange process were achieved at the following speed of the two plasma flow components – $\overrightarrow{v_{pow}} = 25, \overrightarrow{v_g} = 150$ m/s and the value of the Reynolds number, which corresponds to the region of laminar-turbulent transition 11.

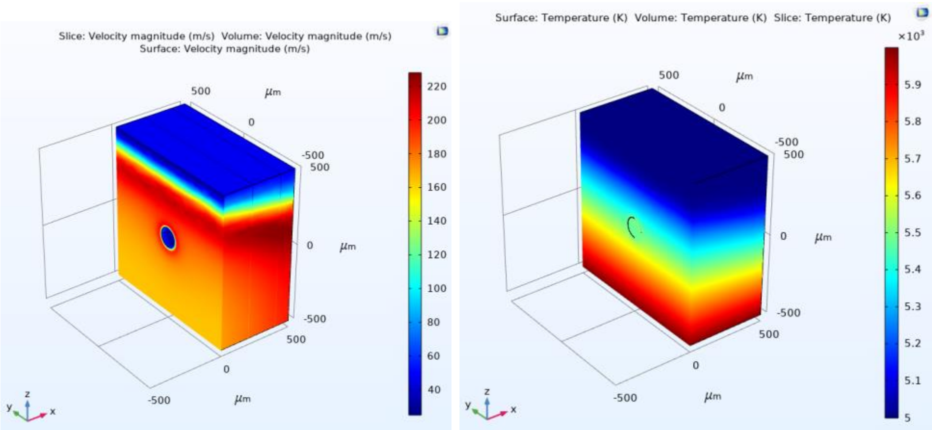

Fig. 3. Typical color maps of flow velocity (left) and
temperature distribution inside the space of the model (right).

Table 2

Thermodynamic subtasks calculation results

Tpar, K				
Vpow/Vg, m/s	**50**	**100**	**150**	**200**
25	5 180	5 100	**5 400**	5 230
50	5 110	5 020	5 340	5 110
75	5 040	4 950	5 290	5 150
100	5 000	5 190	5 230	5 090
Tpar/Tg				
Vpow/Vg. m/s	**50**	**100**	**150**	**200**
25	0.88	0.86	**0.91**	0.88
50	0.86	0.85	0.90	0.86
75	0.85	0.84	0.89	0.87
100	0.85	0.88	0.88	0.86

Analysis of the turbulence influence in the electric arc plasma flow by the laboratory study method

In order to confirm the assumptions, described above, a laboratory experiment was carried out.

Fig. 4. Plasma spraying process.

Metal substrates, made of stainless steel plates of approximately equal dimensions and masses, at fixed technological parameters (as it was described in the part 1) were coated by plasma spraying (detail description of the process is available in the [12–22]). Then the mass gain of the plates was measured for each case, and the values of the Reynolds number, productivity, and process efficiency were calculated.

During the first experiment, the coatings were sprayed at the constant powder supply rate (0.75 g/s) and a variable mass flow rate of the plasma forming gas (as it is shown in the 0). Through the second experiment, the coatings were sprayed at the variable powder supply rate (0.4–0.8 g/s) and a constant mass flow rate of the plasma forming gas equal to 0.75 g/s, which was changed to 1 g/s and 1.4 g/s in the process of the third and fourth experiments. To set the corrections on the increasing amount of the material supplied, an innovative technique was applied – during the experiment of determination the effect on heat transfer of the nature of the movement of gas flows, a mixture of aluminum and low-melting NaCl that does not settle on the substrate 17 was used in each measurement with a proportional content of elements, calculated on the basis of mixture feed rate (*Table* 4).

Based on a formula *(5)*, the value of the heat transfer coefficient α is determined by the following equation:

$$\alpha = \frac{U\cdot I\cdot(n\cdot m/(G))\cdot\eta}{\Delta T\cdot\frac{l_j}{v_p}\cdot S} = \frac{U\cdot I\cdot(m/G)}{\frac{l_j}{v_p}\cdot S\cdot(T/\eta - T)}. \qquad (16)$$

By the values of the mass flow rate of the plasma forming material and formulas (16–19), the values of the velocities of the corresponding flows were obtained.

Table 3

The results and data of the experiment No. 1

P=24000 W, G=0,4 g/s									
G', g/s	**Vg, m/s**	**m1, g**	**m2, g**	**Δm, g**	**W, g/s**	**Vp, m/s**	**Re**	**η, %**	**α, W/(K·m^2)**
0.500	103.821	81.390	82.062	0.672	0.084	144.148	634.586	14.000	14475.005
0.550	114.203	101.114	101.706	0.592	0.074	151.797	668.257	12.333	11975.550
0.600	124.585	103.820	104.364	0.544	0.068	159.754	703.287	11.333	10496.576
0.650	134.967	109.430	109.941	0.511	0.064	167.976	739.484	10.646	9496.186
0.700	145.349	103.190	103.653	0.463	0.058	176.426	776.684	9.646	8298.640
0.750	155.731	101.210	101.632	0.422	0.053	185.073	814.750	8.792	7336.162
0.800	166.113	105.790	106.175	0.385	0.048	193.890	853.566	8.021	6518.479
0.850	176.495	103.760	104.110	0.350	0.044	202.856	893.035	7.292	5789.304
0.900	186.877	103.920	104.243	0.323	0.040	211.951	933.073	6.729	5240.314
0.950	197.259	105.670	105.976	0.306	0.038	221.159	973.610	6.375	4888.983
1.000	207.641	103.190	103.478	0.288	0.036	230.467	1014.586	6.000	4537.130

The flow rate of the substance with a density ρ, mass flow rate G, passing through a section with an area S, is defined by 10:

$$v_n = \frac{G_n}{S_n\cdot\rho_n}. \qquad (17)$$

The total speed of two perpendicular directed streams (v_1, v_2) is defined by the folloeing equation:

$$v = \sqrt{v_1^2 + v_2^2}. \qquad (18)$$

The dynamic system of aluminum particles moving by an air flow can be represented as an equation (for a unit volume and a unit area of space):

$$\overrightarrow{F_{gpow}} = \overrightarrow{F_{pow}} - \overrightarrow{F_p}, \qquad (19)$$

where F_{gpow} is the force, with which the air flow from the dispenser acts on the particle; F_{pow} is the force, with which the particle acts on the oncoming air flow; F_p is the drag force in the considered space.

$$\frac{\rho_{gas}\cdot\overrightarrow{v_{gpow}}^2\cdot S_1}{2} = \frac{\rho_{pow}\cdot\overrightarrow{v_{pow}}^2\cdot S_1}{2} - \frac{1{,}05\cdot\rho_{gas}\cdot S_1\cdot\overrightarrow{v_{pow}}^2}{2}, \qquad (20)$$

where ρ_{gas} is the density of air at room temperature; ρ_{pow} is the aluminum density at room temperature; v_{gpow} is the air flow velocity; $\overrightarrow{v_{pow}}$ is the velocity of the particles; S_1 – unit area, equal to 1; 1.05 – resistance to the drag force in the considered space 10.

Therefore, in the case of moving aluminum particles by an air flow at a known mass flow rate of particles, the air flow velocity is determined by the equations:

$$\overrightarrow{v_{gpow}} = \sqrt{\left(\frac{\rho_{pow}\cdot\left(\frac{G}{S_2\cdot\rho_{pow}}\right)^2 - 1.05\cdot\rho_{gas}\cdot\left(\frac{G}{S_2\cdot\rho_{pow}}\right)^2}{\rho_{gas}}\right)}, \qquad (21)$$

$$\vec{v_p} = \sqrt{v_{gas}^2 + \sqrt{\left(\frac{-\rho_{pow}\cdot\left(\frac{G}{S_2\cdot\rho_{pow}}\right)^2 + 1.05\cdot\rho_{gas}\cdot\left(\frac{G}{S_2\cdot\rho_{pow}}\right)^2}{\rho_{gas}}\right)^2}}, \quad (22)$$

where $\rho_{pow} = \frac{(\frac{Me_{\%}}{100}\cdot\rho_{me}+(1-\frac{Me_{\%}}{100})\cdot\rho_{NaCl})}{2}$ – the density of the supplied powder material (depends on the percentage of metal $Me_{\%}$ in mixture); S_2 – valve area; ρ_{me} is the used metal density at room temperature; ρ_{NaCl} is the salt density at room temperature.

The results of the experiments are presented in the form of graphs (*Fig.* 5). For the cases No. 1, No. 3, no. 4 the dependence was obtained with the character, which is close to logarithmic. The dependence for the case No. 2 has a character, which is close to exponential.

Table 4

The results and data of the experiments No. 2–4.

P = 24000 W, G' = 0.75 g/s										
Al, %	**G, g/s**	**Vgpow, m/s**	**m1, g**	**m2, g**	**Δm, g**	**W, g/s**	**Vp, g/s**	**Re**	**η, %**	**α, W/(K·m^2)**
100.0	0.400	99.278	106.308	106.510	0.202	0.025	193.519	751.703	6.312	10053.859
88.9	0.450	115.389	107.124	107.354	0.230	0.029	202.258	785.649	7.188	10735.295
80.0	0.500	131.813	110.026	110.298	0.272	0.034	212.057	823.713	8.500	12151.513
72.7	0.550	148.498	104.110	104440	0.330	0.041	222.812	865.488	10.313	14366.706
66.7	0.600	165.403	106.102	106.482	0.380	0.048	234.418	910.571	11.875	16237.665
61.5	0.650	182.497	108.666	109.106	0.440	0.055	246.777	958.578	13.750	18667.413
57.1	0.700	199.754	101.380	101.903	0.523	0.065	259.798	1009.158	16.344	22363.573
53.3	0.750	217.152	103.881	104.491	0.610	0.076	273.401	1061.999	19.063	26480.084
50.0	0.800	234.673	103.490	104.260	0.710	0.089	287.515	1116.821	22.188	31606.702
P = 24000 W, G' = 1 g/s										
Al, %	**G, g/s**	**Vgpow, m/s**	**m1, g**	**m2, g**	**Δm, g**	**W, g/s**	**Vp, g/s**	**Re**	**η, %**	**α, W/(K·m^2)**
100.0	0.400	99.278	107.124	107.344	0.220	0.028	201.199	781.536	6.875	11453.072
88.9	0.450	113.725	107.180	107.420	0.240	0.030	208.706	810.698	7.500	11598.254
80.0	0.500	128.754	108.026	108.296	0.270	0.034	217.262	843.929	8.438	12349.767
72.7	0.550	144.417	101.110	101.420	0.310	0.039	226.895	881.348	9.688	13648.201
66.7	0.600	160.774	103.102	103.452	0.350	0.044	237.641	923.090	10.938	15001.775
61.5	0.650	177.892	108.666	109.086	0.420	0.053	249.541	969.315	13.125	17888.862
57.1	0.700	195.852	100.380	100.860	0.480	0.060	262.646	1020.221	15.000	20421.846
53.3	0.750	214.743	103.881	104.431	0.550	0.069	277.019	1076.052	17.188	23643.695
50.0	0.800	234.673	103.490	104.260	0.620	0.078	292.739	1137.115	19.375	27121.446
P = 24000 W, G' = 1.4 g/s										
Al, %	**G, g/s**	**Vgpow, m/s**	**m1, g**	**m2, g**	**Δm, g**	**W, g/s**	**Vp, g/s**	**Re**	**η, %**	**α, W/(K·m^2)**
100.0	0.400	99.278	107.124	107.334	0.210	0.026	209.955	815.547	6.563	11370.086
88.9	0.450	113.725	107.124	107.354	0.230	0.029	217.160	843.534	7.188	11526.251
80.0	0.500	128.754	110.026	110.271	0.245	0.031	225.394	875.520	7.656	11527.397
72.7	0.550	144.417	104.110	104.390	0.280	0.035	234.694	911.643	8.750	12620.137
66.7	0.600	160.774	106.501	106.811	0.310	0.039	245.098	952.058	9.688	13514.579
61.5	0.650	177.892	109.666	110.006	0.340	0.043	256.653	996.941	10.625	14477.560
57.1	0.700	195.852	102.380	102.760	0.380	0.048	269.412	1046.503	11.875	15995.712
53.3	0.750	214.743	103.861	104.281	0.420	0.053	283.443	1101.002	13.125	17609.949
50.0	0.800	234.673	102.490	103.260	0.480	0.060	298.825	1160.753	15.000	20330.539

Results discussion

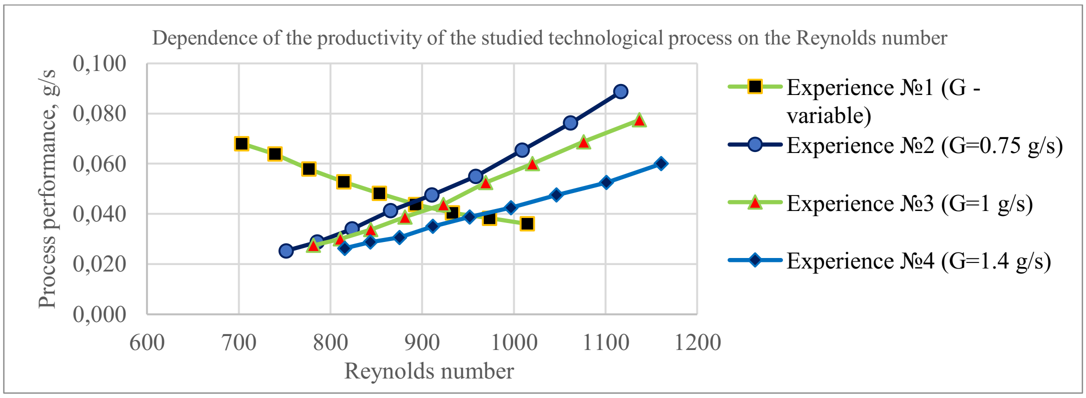

Fig. 5. Comparative research results.

The laboratory study results demonstrate that the decrease in the productivity of the process in the first case is due to the generalized effect of a significant reduction in the trajectory of particles (fixed channel dimensions, fixed position of the plasma torch, reduction in the angle between the flight trajectory and the central axis of the plasma jet) and the increasing of the speed of their movement. This leads to the fact that the time that the particles spent inside the flow becomes insufficient for the melting of particles of a large fraction (50–60 µm), which entails a decrease in the mass gain with an increase in the plasma gas supply rate (longitudinal velocity) 13. At the same time, it should be noted that in the region of the transition of the jet motion nature to the turbulent regime there is a slight decrease in the steepness of the fall of the studied characteristic.

In the case of an increase in the feed rate of the powder material (transverse velocity), the trajectory of the particles increases, which entails an increase in the amount of time that the particles stay in the plasma jet 23, which together with a positive effect of the nature of flow movement transition to turbulent character (in the region of the jet movement nature transition to turbulent regime there is a sharp enhance in the steepness of the increase in the characteristic under study) confirms the assumption that the property of heat transfer improves in the region of the laminar-turbulent transition. The influence of the magnitude of the longitudinal and transverse components of the plasma flow velocity 24 was demonstrated in mathematical model, which was presented by our team in 13.

To conformation of the assumptions, which were made earlier, an additional experiment was carried out – the reiteration of the experiments No. 2–4 with the replacement of the aluminum metal powder with a higher density material (Ni_3Al) for which, theoretically, it is possible to improve the trajectory of motion in the plasma flow with an absolutely identical material supply parameters, as in the previous experiments, associated with the expected positive effect of the free fall acceleration value increase for each particle (to an acceptable extent, which should allow increasing the time that a particle spent inside the flow without vertical escape). Calculations (*Table* 5) were supplemented by the parameter α check with the formula, which is based on the Nusselt number value 9:

$$Nu = 2 + 0.6 \cdot Re^{0,5} Pr^{0,33}\,, \qquad (23)$$

$$\alpha_{Nu} = \frac{Nu \cdot (\lambda_{300} + \lambda_{6000})}{2 \cdot d_s}\,, \qquad (24)$$

where Nu – the Nusselt number, λ_{300} and λ_{6000} – thermal conductivity of the material at the temperature equal to 300 and 6 000 K.

As expected, as a result, the dependencies of a similar nature were obtained, and the process productivity was increased by almost 1.5 times for the first plasma spraying configuration.

The correlation of the values of the heat transfer coefficient found by the various methods can become the subject of long discussions 25, since, from the standpoint of conformism 26, it demonstrates the inconsistency of the formula *(16)*. On the other hand, due to the fact that the measurements were carried out in the poorly studied region of the laminar-turbulent transition 27, that obtained relations between the values α и α_{Nu} for each experiment got the different kinds of dependences between each other, the fact that the order of these values approximately coincides, and, furthermore, the fact that for the experiment No. 6 this values are approximately identical, we, trying ourselves on the role of innovators, have the moral right to believe that the developed concept can be realistic.

On the basis of the results of the laboratory study, we can make an unambiguous conclusion – the turbulent nature of the plasma flow positively affects on the heat exchange between plasma and powder. The most optimal parameters of plasma spraying processes are:

- increased residence time of powder material inside the plasma jet, achieved by increasing of the movement trajectory, by the regulations of the longitudinal component of the flow velocity within certain limits, which require additional research to be found;
- the largest value of the Reynolds number, which corresponds to the first condition (and as it seen – it is sets in the range of values, corresponding to the laminar-turbulent transition area).

Table 5

The results and data of the experiments No. 5–7

Ni3Al, %	G, g/s	Vgpow, m/s	m1, g	m2, g	Δm, g	W, g/s	Vp, m/s	Re	η, %	α, W/(K·m^2)	αNu, W/(K·m^2)
P=24000 W, G'= 0.75 g/s											
100.0	0.400	59.575	104.526	105.041	0.515	0.064	176.473	685.491	16.094	72532.831	59994.261
88.9	0.450	70.456	104.122	104.699	0.577	0.072	180.437	700.889	18.031	75603.904	60184.816
80.0	0.500	81.798	108.023	108.657	0.634	0.079	185.161	719.237	19.813	78426.837	60409.165
72.7	0.550	93.560	103.320	104.043	0.723	0.090	190.649	740.555	22.594	86723.532	60666.263
66.7	0.600	105.704	106.432	107.810	0.778	0.097	196.893	764.810	24.313	90352.028	60954.324
61.5	0.650	118.200	108.666	109.479	0.813	0.102	203.874	791.927	25.406	91567.246	61271.018
57.1	0.700	131.019	100.650	101.535	0.885	0.111	211.564	821.799	27.656	99035.217	61613.662
53.3	0.750	144.137	103.940	104.882	0.942	0.118	219.930	854.293	29.438	104858.228	61979.396
50.0	0.800	157.533	111.450	113.040	0.990	0.124	228.933	889.265	30.938	109878.842	62365.328
P = 24000 W, G' = 1 g/s											
Ni3Al, %	**G, g/s**	**Vgpow, m/s**	**m1, g**	**m2, g**	**Δm, g**	**W, g/s**	**Vp, m/s**	**Re**	**η, %**	**α, W/(K·m^2)**	**αNu, W/(K·m^2)**
100.0	0.400	59.575	101.250	101.620	0.370	0.046	184.863	718.080	11.563	51791.430	60395.097
88.9	0.450	70.456	107.180	107.573	0.393	0.049	188.651	732.793	12.281	50309.393	60573.088
80.0	0.500	81.798	108.026	108.460	0.434	0.054	193.173	750.362	13.563	51959.887	60783.289
72.7	0.550	93.560	101.110	101.597	0.487	0.061	198.440	770.819	15.219	55513.558	61024.980
66.7	0.600	105.704	105.910	106.440	0.530	0.066	204.447	794.151	16.563	57975.737	61296.741
61.5	0.650	118.200	108.666	109.242	0.576	0.072	211.178	820.298	18.000	61128.990	61596.605
57.1	0.700	131.019	100.380	100.981	0.601	0.075	218.611	849.172	18.781	61900.760	61922.230
53.3	0.750	144.137	103.881	104.507	0.626	0.078	226.717	880.657	19.563	63014.631	62271.052
50.0	0.800	157.533	103.680	104.330	0.650	0.081	235.461	914.621	20.313	64306.464	62640.425
P = 24000 W, G' = 1.4 g/s											
Ni3Al, %	**G, g/s**	**Vgpow, m/s**	**m1, g**	**m2, g**	**Δm, g**	**W, g/s**	**Vp, m/s**	**Re**	**η, %**	**α, W/(K·m^2)**	**αNu, W/(K·m^2)**
100.0	0.400	59.575	103.950	104.220	0.270	0.034	194.356	754.955	8.437	38378.429	60837.839
88.9	0.450	70.456	104.514	104.796	0.282	0.035	197.962	768.963	8.813	36440.718	61003.186
80.0	0.500	81.798	105.214	105.509	0.295	0.037	202.277	785.723	9.219	35213.207	61199.048
72.7	0.550	93.560	103.660	103.964	0.304	0.038	207.312	805.283	9.500	33914.935	61425.003
66.7	0.600	105.704	104.100	104.418	0.318	0.040	213.069	827.644	9.938	33585.767	61679.976
61.5	0.650	118.200	104.331	104.666	0.335	0.042	219.536	852.765	10.469	33850.589	61962.358
57.1	0.700	131.019	103.210	103.563	0.353	0.044	226.696	880.575	11.031	34417.992	62270.150
53.3	0.750	144.137	100.810	101.177	0.367	0.046	234.522	910.975	11.469	34721.201	62601.101
50.0	0.800	157.533	101.147	101.530	0.383	0.048	242.985	943.849	11.969	35396.029	62952.828

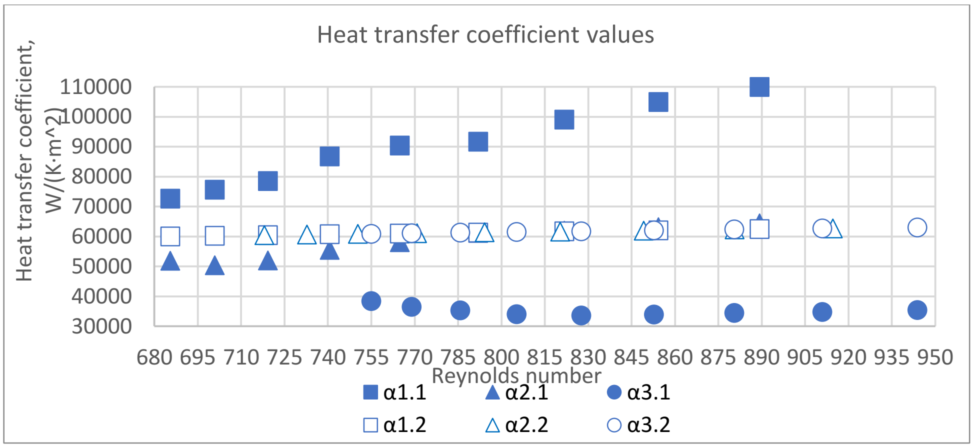

Fig. 6. Heat transfer coefficient values obtained by various methods.

Conclusions

The results of laboratory and mathematical experiments indicate the positive influence of the turbulent nature of the gaseous environment movement presence on the value of the heat transfer coefficient α; however, the optimal operating modes of plasma torches in the process of plasma spraying should take into account the need for the particles to be melted in the plasma flow for a certain time (sufficient to melt the largest-fraction particles which used). Discovered through the research the fact that the optimal configurations are the ones with the transitional nature of the movement of plasma flow – working in the laminar-turbulent transition area – with a few more evidences may become the basis of the new paradigm for the plasma spraying systems applications optimization and make a breakthrough in this technology.

On the basis of the correlation of the results of mathematical and laboratory experiments, in the first approximation, the optimal ratio of the plasma forming gas and the powder material feeding flow rates is equal to 1:1.5.

On the basis of the results of the study, it becomes clear that the installation dimensions (nozzle cross section, channel length) also have a large degree of influence on the processes under consideration. In order to find the most optimal particle trajectories, it is necessary to perform a series of additional experiments that takes into account the channel geometry, the distance to the substrate and modernize the main equations, by the adding of the more accurate velocity calculations.

The study was carried out within the framework of the research topic under the state assignment of Ministry of Science and Higher Education of the Russian Federation “FSEG-2023-0012”.

REFERENCES

1. Балдаев Л. Х., Борисов В. Н. и др. Газотермическое напыление: учеб. пособие под общ. ред. Л. Х. Балдаева. М.: Маркет ДС, 2007. 344 с. [Baldaev L. Kh., Borisov V. N. et al. Gas-thermal spraying. Textbook. Ed. L. H. Baldaev. M.: Market DS. 2007. 344 p.].
2. Фролов В. Я. и др. Электротехнологические промышленные установки: учеб. пособие / под ред. В. Я. Фролова. Федеральное агентство по образованию, Санкт-Петербургский гос. политех. ун-т. СПб.: изд-во Политехнического ун-та, 2010. 571 с. [Frolov V. Ya. et al. Electrotechnological industrial installations: textbook / ed. V. Ya. Frolov. Federal Agency for Education, St. Petersburg State Polytechnic University. St. Petersburg: publishing house of the Polytechnic University. 2010. 571 p.].
3. Руткаускас Т. К. и др. Экономика организации (предприятия): учеб. пособие. Рекомендовано методическим советом Уральского федерального университета для студентов вуза, обучающихся по направлениям подготовки 38.03.01 – Экономика, 38.05.01 – Экономическая безопасность / под общ. ред. Т. К. Руткаускас; Министерство образования и науки РФ, Уральский федеральный университет им. первого Президента России Б. Н. Ельцина. 2-е изд-е, перераб. и доп. Екатеринбург: ООО «Изд-во УМЦ УПИ», 2018. 260 с. [Rutkauskas T. K. et al. Economics of an organization (enterprise): textbook. Recommended by the methodological council of the Ural Federal University for university students studying in the areas of training 38.03.01 – Economics, 05.38.01 – Economic security / ed. T. K. Rutkauskas. Ministry of Education and Science of the RF, Ural Federal University named after the first President of Russia B. N. Yeltsin. 2nd ed., rev. and exp. Yekaterinburg: UMC UPI Publishing House LLC. 2018. 260 p.]
4. Bauchire J. M., Gonzalez J. J. & Gleizes A. Modeling of a DC Plasma Torch in Laminar and Turbulent Flow. Plasma Chemistry and Plasma Processing, Vol. 17. 1997. Pp. 409–432. URL: https://doi.org/10.1023/A:1021847113956
5. Cheng K., Chen X. & Pan W. Comparison of Laminar and Turbulent Thermal Plasma Jet Characteristics – A Modeling Study. Plasma Chem Plasma Process. 2006. Vol. 26. Pp. 211–235. URL: https://doi.org/10.1007/s11090-006-9006-6
6. Энгельшт В. С., Гурович В. Ц., Десятков Г. А. и др. Низкотемпературная плазма. Теория столба электрической дуги / под ред. Жукова М. Ф. Новосибирск: Наука. Сиб. отд-ние, 1990. Т. 1. 376 с. [Engelsht V. S., Gurovich V. Ts., Desyatkov G. A. et al. Low temperature plasma. The theory of the electric arc column / ed. M. F. Zhukova. Novosibirsk: Science. Sib. department. 1990. Vol. 1. 376 p.].
7. Кудинов В. В., Бобров Г. В. и др. Нанесение покрытий напылением. Теория, технология и оборудование. В. В. Кудинов М.: Металургия. 1992. 432 с. [Kudinov V. V., Bobrov G. V. et al. Spray coating. Theory, technology and equipment. M.: Metallurgy. 1992. 432 p.].
8. Фролов В. Я., Клубникин В. С., Петров Г. К., Юшин Б. А. Техника и технологии нанесения покрытий: учеб. пособие. СПб.: изд-во Политехн. ун-та. 2008. 307 с. [Frolov V. Ya., Klubnikin V. S., Petrov G. K., Yushin B. A. Technique and technology of coating. Textbook. St. Petersburg: Politekh. Univ. 2008. 307 p.].
9. Дресвин С. В., Зверев С. Г. Теплообмен в плазме: учеб. пособие. СПб.: изд-во Политехн. ун-та. 2008. 212 с. [Dresvin S. V., Zverev S. G. Heat exchange in plasma: textbook. St. Petersburg: Politekh. Univ. 2008. 212 p.].
10. Дресвин С. В., Донской А. В., Гольдфарб В. М., Клубникин В. С. Физика и техника низкотемпературной плазмы / под общ. ред. С. В. Дресвина. М.: Атомиздат. 1972 [Dresvin S. V., Donskoy A. V., Goldfarb V. M., Klubnikin V. S. Physics and technology of low-temperature plasma / ed. S. V. Dresvina. M.: Atomizdat. 1972].
11. Дресвин С. В., Иванов Д. В. Физика плазмы: учеб. пособие. СПб: изд-во Политехн. ун-та, 2013. 544 с. [Dresvin S. V., Ivanov D. V. Plasma physics: textbook. St. Petersburg: Polytech. Univ. 2013. 544 p.].
12. Derevyankin P. G., Kriskovets D. S., Frolov V. Y., Yushin B. A. Analysis of the electrophysical and thermophysical properties of copper-graphite material for arcing contacts of a high-current low-voltage circuit breaker // Proceedings of the 2021 IEEE Conference of Russian Young Researchers in Electrical and Electronic Engineering, ElConRus 2021. 2021. Pp. 839–843.
13. Petrenya Y. K., Frolov V. Y., Kriskovets D. S., Yushin B. A., Ivanov D. V. The Influence of Electric Arc Plasma Turbulence on Heat Transfer Processes Involving Powder Materials. Energies, 2023. Vol. 16. 5632. URL: https://doi.org/10.3390/en16155632
14. Lima R. S., Li H., Khor K. A., Marple B. R. Biocompatible Nanostructured High-Velocity Oxyfuel Sprayed Titania Coating: Deposition, Characterization and Mechanical Properties. J. Therm. Spray Technol, 2006. Vol. 15. Pp. 623–627.
15. Huang R., Fukanuma H., Uesugi Y., Tanaka Y. Simulation of Arc Root Fluctuation in a DC non-Transferred Plasma Torch with Three Dimensional Modeling. J. Therm. Spray Technol. 2012. Vol. 21. Pp. 636–643.
16. Tradia A. Multiphysics Modeling and Numerical Simulation of GTA Weld Pools. Ph.D. Thesis. Ecole Polytechnique, Paris. 2011. 224 p.
17. Amouroux J., Morvan D., Ouvrelle L., Dresvin S., Ivanov D., Zverev S., Feigenson O., Balashov A. Calculation of silicon particles dynamics, heat and mass transfers in thermal plasmas. Effect of particles vaporization. High Temp. Mat. Proc. 2003. Vol. 7. Pp. 93–105.
18. Colombo V., Concetti A., Ghedini E. Time dependent 3D large eddy simulation of a DC non-transferred arc plasma spraying torch with particle injections. Proceedings of the 2007 16th IEEE International Pulsed Power Conference. Albuquerque, 17–22 June 2007. Vol. 2. Pp. 1565–1568.
19. Trelles J. P., Chazelas C., Vardelle A., Heberlein J. V. R. Arc plasma torch modeling. J. Therm. Spray Technol, 2009. Vol. 18. Pp. 728–752.

20. Williamson E. H., Gee M., Robertson D., Watts J. F., Whiting M. J., Yeomans J. A. A comparative study of the wear performance of hard coatings for nuclear applications. Wear. 2022. Vol. 488–489.
21. Cannon K. M., Dreyer C. B., Sowers G. F., Schmit J., Nguyen T., Sanny K., Schertz J. Working with lunar surface materials: Review and analysis of dust mitigation and regolith conveyance technologies. Acta Astronautica, 2022. Vol. 196. Pp. 259–274.
22. Memon H., Romero A. R., Derelizade K., Venturi F., Hussain T. A new hybrid suspension and solution precursor thermal spray for wear-resistant silicon carbide composite coatings. Materials & Design. Vol. 224. 2022.
23. Boulos M. I., Fauchais P. L., Pfender E. Handbook of Thermal Plasmas. Springer International Publishing: Cham. 2023. 1973 p.
24. Robert E., Sarron V., Darny T., Riès D., Dozias S., Fontane J., Joly L. and Pou-vesle J. M. Rare gas flow structuration in plasma jet experiments. Plasma Sources Science and Technology, 2014. Vol. 23(1).
25. Iséni S., Schmidt-Bleker A., Winter J., Weltmann K.-D., Reuter S. Laminar versus turbulent flow of an argon rf appj investigated by oh plif and its influence on the discharge propagation, 2014.
26. Morabit Y., Whalley R., Robert E., Hasan M., Walsh J. Turbulence and entrainment in an atmospheric pressure dielectric barrier plasma jet. Plasma Processes and Polymers, 2019. Vol. 17.
27. Solonenko O. P., Fedorchenko A. I. (Eds.). Plasma Jets in the Development of New Materials Technology: Proceedings of the International Workshop. Frunze. September 1990. 1st ed. CRC Press. 1990. URL: https://doi.org/10.1201/9780429070938.

Received 17.09.2023.